CONF-801068--24

CONF-801068--24

DE88 012120

APPENDIX C

Angular Scattering In Electron Capture and Loss D^- Beam Formation Processes

M. J. Coggiola, R.V. Hodges, D. L. Huestis, and J. R. Peterson

This paper was presented at the Second International Symposium on the Production and Neutralization of Negative Hydrogen Ions and Beams at Brookhaven National Laboratory, October 1980

DISCLAIMER

Conference on Negative Ion Beams
6-10 October 1980
Brookhaven National Lab, N.Y.

ANGULAR SCATTERING IN ELECTRON CAPTURE AND LOSS D^- BEAM FORMATION PROCESSES

M. J. Coggiola, R. V. Hodges, D. L. Huestis
and J. R. Peterson
Molecular Physics Laboratory, SRI International
Menlo Park, California 94025

Abstract

The development of high energy (>150 keV) neutral beams for heating and fueling magnetic fusion devices depends on the ability to produce well-collimated negative ion beams. The double capture charge-exchange technique is a known, scalable method. In order to maximize the overall efficiency of the process and to achieve the desired beam characteristics, it is necessary to examine the optical qualities of the beams as well as the total efficiency of beam production. A combined modeling and experimental study of the angular scattering effects in negative ion formation and loss processes has therefore been undertaken.

Introduction

A program has recently been initiated to enable the modeling of D^- beam formation by the "double capture" method, including the attendant angular scattering which can have a strong effect on the optical quality and usefulness of the beam. In addition to the development and use of the model, the effort includes experimental measurements of angular differential and total cross sections required for the model's data base. This approach uses either experimental or theoretical input data for single collision cross sections, and allows predictions of optimum beam energy and target thickness to maximize the optical properties as well as the total yield of the beam for any target species.

In the following sections, we will outline the mathematical model used to describe the double charge exchange negative ion production process, and discuss the available experimental and theoretical input data and the preliminary results of the modeling. The second section of this report will describe the experimental apparatus used for cross section measurements. Finally, some preliminary experimental data will be presented and discussed.

Modeling of D^- Production

A computer model has been developed to calculate the angular distributions of the various charge species in a double charge exchange D^- source as a function of target thickness. The computations are carried out on the PDP 11/40 computer, and the graphical results are displayed on and copied from a video terminal. The model uses Legendre series expansions in the manner of multiple scattering theory.[1] We presently ignore excited states, assuming that the metal vapor target atoms are in the ground state, and that the excited D^0 states produced in (+o) collisions are rapidly quenched by radiation, stray electric fields or collisions before another angle-changing collision occurs. For each charge state $i = +, o, -$, the angular distribution $C_i(\theta,x)$ at a given thickness (line density) x (cm^{-2}) is expressed as

$$C_i(\theta,x) = \frac{1}{4\pi}\sum_n (2n+1) b_n^i(x) P_n(\cos\theta). \qquad (1)$$

The nine elastic and inelastic angular differential cross sections $\sigma_{ij}(\theta)$, are similarly expanded as

$$\sigma_{ij}(\theta) = S_{ij}\cdot\frac{1}{4\pi}\sum_n (2n+1) f_n^{ij} P_n(\cos\theta), \qquad (2)$$

where the total cross sections are

$$S_{ij} = 2\pi\int_o^\pi \sigma_{ij}(\theta)\sin\theta d\theta. \qquad (3)$$

In solving the multiple collision case, the use of the Legendre expansion is particularly useful because it separates the partial waves of the distribution so that in a charge-changing collision each partial wave n from the initial distribution scatters into the same n in the next. Thus, after part of a beam of + ions, whose angular distribution $C_+(\theta,x)$ has expansion coefficients b_n^+, undergoes one charge transfer collision of cross section σ_{+o}, with expansion coefficients f_n^{+o}, the angular distribution of the resulting neutrals is characterized by coefficients $b_n^o = b_n^+ f_n^{+o}$. Multiple scattering is thus rather easily treated by an iterative procedure.

The evolution of the angular distributions as the beams pass through the target is represented by the rate equations for the expansion coefficients

AT03-80ER53091

$$\frac{db_n^i}{dx}(x) = S_{ii}(1-f_n^{ii})b_n^i(x) + \sum_{k\neq i}^{m}[S_{ki}f_n^{ki}b_n^k(x) - S_{ik}b_n^i(x)] , \qquad (4)$$

where the first term represents elastic scattering and the terms inside the brackets represent charge-changing collisions into and out of the i^{th} charge state.

This is a linear, first-order, homogeneous system of differential equations with constant coefficients which can be represented formally by

$$\frac{d}{dx}\vec{b}_n(x) = -\vec{b}_n(x)\hat{D}_n \qquad (5)$$

where $\vec{b}_n$ is the row vector (b_n^+, b_n^o, b_n^-), and $\hat{D}_n$ is a "decay" matrix with elements

$$D_n^{ii} = S_{ii}(1-f_n^{ii}) + \sum_{k\neq i} S_{ki}, \quad D_n^{ij} = -S_{ij}f_n^{ij}.$$

We solve this system of differential equations as an eigenvalue problem. Hooper and Willman[2] followed a similar approach for the angular scattering due only to the charge-changing collisions between the o and - states neglecting elastic scattering. In that two-state problem, the matrix equations are solvable explicitly.

In order to expand the cross sections in a Legendre series we first expand their angles by 10 so that 18^o maps into 180^o. This expansion reduces the number of terms n required for a fit. We then approximate the cross sections by a least-squares fit to an approximately Gaussian expansion

$$\sigma_{ij}(\theta) \simeq \sum_k A_{ij}^k \exp[-\alpha_{ij}^k(1-\cos\theta)] . \qquad (6)$$

A satisfactory fit is generally found using only five terms (k = 1-5) with α_{ij}^k covering a wide dynamic range, e.g.,:8,32,124,512,1024. Fig. 1 shows such a fit to the $\sigma_{o-}(\theta)$ data of Cisneros et al.[3] for $D+Cs \rightarrow D^- + Cs^+$ at 500 eV.

Although there has been considerable experimental work on negative ion production from H^+ and D^+ beams in metal vapors, almost all of it has considered only the total charge fraction yields as functions of energy and target thickness, with almost no data being available on angular distributions. Most work has been done on Cs, but even here only $\sigma_{o-}(\theta)$ has been measured for 500 eV ≤ E ≤ 2500 eV by Cisneros et al.[3] and

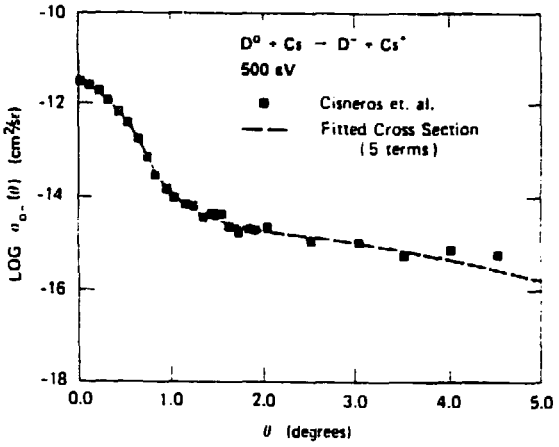

Fig. 1 Least squares fit (---) of a 5 term expansion of Eq. (6) to the σ_{o-} data (■) of Cisneros et al. (Ref. 4).

the relative values of σ_{oo} have been determined by Pradel, Maddarsi and Valance[4] at 30 eV < E < 528 eV. In order to test our model, we considered 500 eV D^+ + Cs, using the Cisneros data for σ_{o-} and the relative σ_{oo} of Pradel et al. for all elastic cross sections, arbitrarily scaled to yield total S_{ii} that were considered reasonable. The absolute values of σ_{+-} reported by Cisneros et al. display a dependence on x even at their lowest pressures, thus their quoted $S_{+-} = 1 \times 10^{-16}$ cm^2 is probably too high. We used their σ_{+-} angular dependence but set $S_{+-} = 2 \times 10^{-17}$, which is near the value of 1.4×10^{-17} cm^2 derived by Hooper et al.[5] Other angular distributions were estimated, and the magnitudes of the σ_{ij} were chosen to yield the total cross sections S_{ij} given in Table 1. Figure 2 shows the fitted angular scattering cross sections used to test the model.

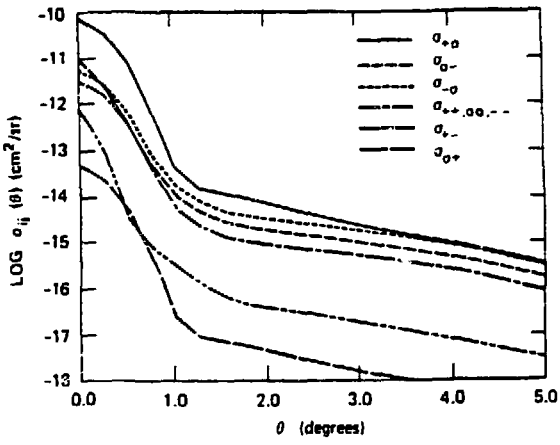

Fig. 2 Computer generated fits to σ_{ij} differential cross sections used in the modeling studies.

Table I Summary of total cross section values used for model testing. All cross sections are for $D^{+,o,-}$ + Cs at 500 eV collision energy.

S_{ij}	MI[a]	HWS[b]	Meyer[c]	MII[d]
+o	7.5(-15)[e]	1.1(-14)	1.5(-14)	1.6(-14)
o+	4.7(-18)	1.4(-17)		4.7(-18)
o-	3.5(-16)	4.5(-16)	8.5(-16)	4.5(-16)
-o	6(-16)	8.8(-16)	4.2(-15)	8.8(-16)
+-	2(-17)	1.4(-17)		1.5(-17)
-+	0			0
++	5(-16)			2.5(-15)
oo	5(-16)			2.5(-15)
--	5(-16)			5(-15)

[a]MI values were used to generate all model results shown in this report.
[b]HWS: Hooper et al., Ref. 5.
[c]Meyer: Ref. 6.
[d]MII values for elastic scattering and +o are thought to be more realistic.
[e]7.5(-15) = 7.5×10^{-15} cm^2.

The total fractional yields computed from the model (integrated over all θ) versus energy are shown in Fig. 3. They are similar but not identical to those of Schlachter, Stalder, and Stearns[7] because the S_{ij} are not quite the same. (The elastic S_{ii} do not enter here.) An example of the relative angular intensities of D^o and D^- is shown in Fig. 4 for a line density $x = 1 \times 10^{14}$ cm^{-2}. At this x, the D^o and D^- fractions are about 0.5 and 0.1, respectively, and the D^- angular distribution is still broader than D^o, reflecting the two step process. As x increases, the increased shuttling between the o and - charge states equalizes the angular distributions as the intensities approach their equilibrium value. The distributions continue to broaden, due to both elastic and charge-transfer scattering. For this first trial case, the elastic σ_{ii} were all set equal and $S_{ii} = 5 \times 10^{-16}$ cm^2. The angular distributions (from Pradel et al.[4]) are probably reasonable for σ_{oo} but, judging from recent calculations on D + Na by Olson,[8] S_{oo} should be about 10x larger. Our measurements will soon provide realistic values for these cross sections. Probably all S_{ii} are too small in our example, and thus the angular effects in this illustrative example are unrealistically small. Plots similar to Fig. 4 are easily obtained for any x.

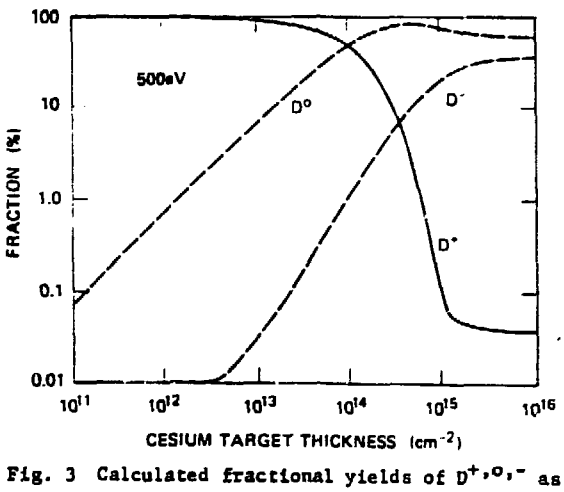

Fig. 3 Calculated fractional yields of $D^{+,o,-}$ as a function of Cs target thickness.

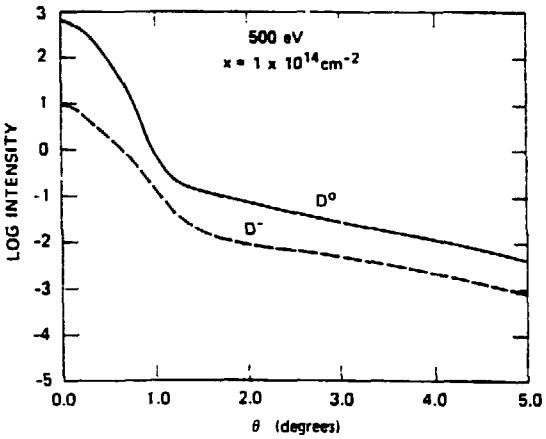

Fig. 4 Model generated angular distributions of the relative intensities of D^o and D^- for a Cs line density of 1×10^{14} cm^{-2}.

Figure 5 shows plots of the integrated o and - fractions of the beam as a function of beam angle for $x = 2 \times 10^{15}$ cm^{-2}, where the charge fractions are close to their equilibrium values. This graph only extends to θ = 1° to show the small angle yields. The 50%, 90%, and 100% values of the total yield at this x are also drawn in by the computer. Their intersections with the angular integrated yield curves show that the 50% angle for D^- is $\theta^-_{0.5} = 0.57°$, and for D^o, $\theta^o_{0.5} = 0.43°$. Similarly, $\theta^-_{0.9} = 1.8°$ and $\theta^o_{0.9} = 1.0°$. A more realistic choice of cross sections given in column 4 of Table I yields $\theta_{0.5} \simeq 3°$ for both charge states at $x = 2 \times 10^{15}$ cm^{-2}. As x increases so that many collisions occur, the angular spreads tend to increase as $x^{\frac{1}{2}}$, as pointed out by Hooper et al.[9] A plot of the 50% and 90% angles is shown in Fig. 6, along with the values of Cisneros,[3] Hooper,[9] and Agafonov.[10] The model's approach to an $x^{\frac{1}{2}}$ behavior at large x is apparent. At midvalues of x, a flattening occurs representing the two-step (+o,o-) convolved cross section, and then at lower x ($< 10^{15}$ cm^{-2}) the angle decreases toward the single step (+-) scattering result which is given by value of the Cisneros points at $x = 3 \times 10^{13}$ cm^{-2}. Their "thin target"

value should be plotted at $x \leq 10^{13}$ cm^{-2} because of the density dependence effects mentioned above.

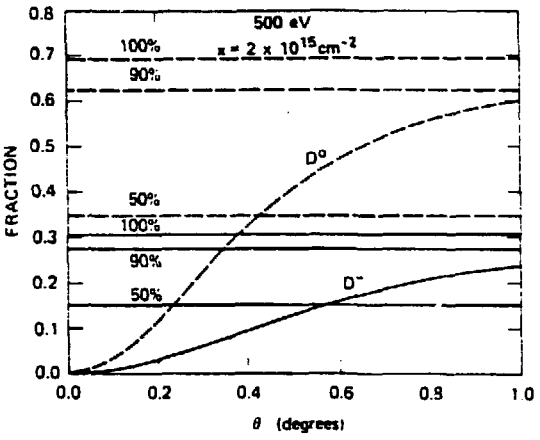

Fig. 5 Fractions of D^0 and D^- within a beam whose angular width is θ, calculated for $x = 2 \times 10^{15}$ cm^{-2}.

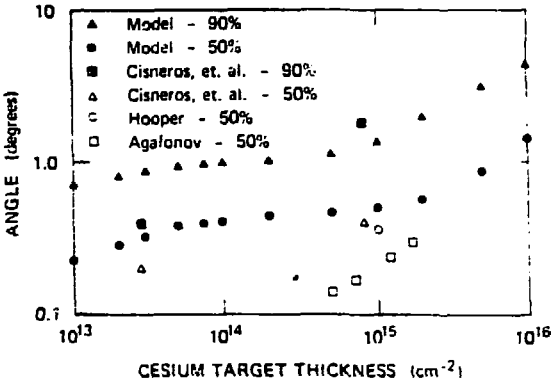

Fig. 6 50% (•) and 90% (▲) angles for D^- production as a function of Cs target thickness. Experimental values: (■,△) Ref. 3, (○) Ref. 8, (□) Ref. 9.

The $\theta_{\frac{1}{2}}$ results of Agafonov et al.[10] are lower than the other results perhaps because of the way they subtracted out the angular spread of the incident beam. Preliminary measurements of the σ_{0-} angular distribution in our lab (see below) agree well with the results of Cisneros et al., which are used in the model. However, we have not yet deconvoluted the incident beam profile, so it is possible that our σ_{0-} is too broad. This cross section introduces the most angular scattering at $10^{13} < x < 10^{15}$ cm^{-2}.

The model provides a powerful tool for examining the relative importance of different processes in the overall performance of double-capture D^- beam sources. It provides an insight and detail that is difficult to obtain from fractional yield measurements alone. Its future use is critically dependent on the required input data that must be provided by experiment or theory. On the other hand, for modeling purposes the differential cross sections can be represented as smooth functions of angle, and the S_{ij} are generally smooth functions of energy, therefore the number of energies required for the input data is reasonably limited.

Experimental

Supplementing the modeling effort is a companion experimental program to supply input data required by the model. As mentioned above, the differential scattering cross sections for most of the elastic and inelastic (charge-changing) collisions are presently unknown, despite their importance in determining an optimal negative ion source design. Furthermore, only a few total cross sections have been measured at energies below 0.5 keV/amu. Thus, our experimental program is designed to measure both total and differential scattering cross sections of $D^{+,0,-}$ in metal vapor targets at low collision energies.

A brief description of the apparatus will be given below, including its unique features and capabilities. In the final section, some preliminary cross section results will be presented.

The scattering apparatus is of straightforward design, and consists of three separately pumped vacuum regions: (1) ion source, (2) charge-exchange neutralization cell, (3) metal vapor target cell and differential detectors. For producing D^+ or D^0 incident beams, a dc discharge type ion source is employed. In either case, positive ions are directly extracted from a discharge formed in pure D_2. The ion beam is accelerated, focussed, and magnetically mass analyzed to yield a pure D^+ beam. For D^- experiments, a duoplasmatron type ion source is used.

The second vacuum region contains a 10 cm long neutralization cell located just downstream from a 1 mm diameter collimating aperture. To produce a ground state D^0 atom beam, a suitable gas such as Ar is admitted to the neutralizing cell, and residual ions are removed at the exit. The neutralization cell can also be filled with alkali metal vapor, thus allowing for the production of D(2S) atoms.

The scattering (target) cell itself is located in the final chamber immediately downstream from a second 1 mm diameter aperture. The two 1 mm apertures, located 35 cm apart, produce an angular collimation at the target of $\sim 0.15°$.

The all stainless-steel target cell has a central well which serves as both the Cs reservoir and the scattering region. The entire cell is uniformly heated by tantalum wire heating elements which run the full vertical length of the unit. Additional elements are provided to heat the interchangeable entrance and exit apertures separately. These apertures, separated by 2.5 cm, consist of a 1.25 mm diameter circular entrance aperture and a 1.5 x 10 mm exit slit. This arrangement allows in-plane scattering out to $\pm 10^{\circ}$ to be observed. Two thermocouples are inserted into deep wells in the body of the cell, one accurately monitors the temperature, while the other is used with a set-point controller to regulate the temperature to $\pm 0.1^{\circ}$C. The entire assembly is mounted on a tilting mechanism which allows the cell to be moved into and out of the incident beam path. A cam system is used to locate the cell with a positional accuracy of ± 0.1 mm, thus ensuring reproducible alignment of the cell apertures with the fixed collimating apertures. No measurable change in the transmitted beam intensity occurs when the evacuated oven is moved into the beam path. This target in-out system simplifies accurate total attenuation cross section measurements and also allows background corrections to be made easily in differential experiments.

For total attenuation measurements, a large aperture ($\pm 8^{\circ}$ acceptance angle) Faraday cup is used to determine the beam flux. For neutral beams, detection is via secondary electron emission. Since a total attenuation method is used, no absolute detection sensitivities need be known to obtain total cross sections. Angular scattering distributions are observed using a detector which rotates about the center of the target cell. It consists of a 1 mm diameter defining aperture followed by a set of deflector plates for charge separation, and finally three separate, shielded detectors. Two channeltron electron multipliers and a suppressed Faraday cup are used as detectors, depending on the type of measurement being made. The overall angular resolution of the detector system is calculated to be $\sim 0.2^{\circ}$.

The measurement of absolute total cross sections requires a knowledge of the true target thickness, $x = \int n(\ell)d\ell$. Rather than determining this parameter by relying on the usual temperature-vapor pressure curves and the measured cell length, we have made use of previously measured absolute charge-exchange cross sections for $He^+ + Cs$.[11] It is a simple matter to measure the attenuation of a He^+ beam at a fixed cell temperature and thereby to determine the effective target thickness at that temperature. This calibration procedure is typically carried out at several He^+ beam energies between 0.3 and 1.5 keV for each cell temperature used. In general, we find that the value of x thus determined is within $\pm$ 5% of the value one would calculate from the measured cell temperature and length.

Initially, we have focused attention on measurements of both the total and differential cross sections for $D^+ + Cs \rightarrow D^0 + Cs^+$. A number of previous measurements have been made of the total cross section for this process at energies above 0.5 keV/amu. Therefore, this system can serve to check the overall performance and calibration of the apparatus.

Figure 7 shows the results of our S_{+o} determinations made using the attenuation technique over a range of collision energies from 0.1 to 2 keV/amu. The cross sections at each energy were measured for several different Cs target densities and averaged together to yield the data shown. The error bars represent the statistical variation in the results as determined from the separate measurements. Day-to-day variations in the measured cross sections were always less than these error limits.

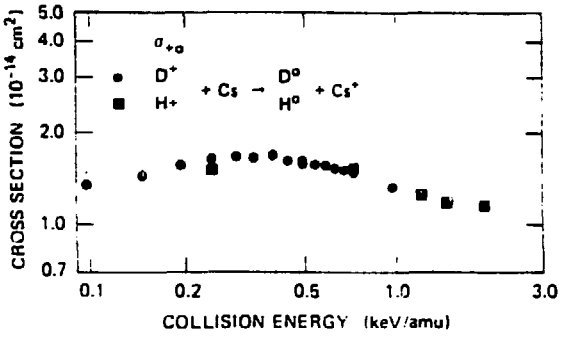

Fig. 7 Experimental total (+o) cross sections for D^+(•) and H^+ (■) charge-exchange in Cs ($x = 1.1 \times 10^{13}$ cm^{-2}) as a function of collision energy.

The cross sections appear to have a broad maximum around 0.4 keV/amu, with a 10-25% decrease at lower and higher energies. This general behavior has been observed previously for this system, both experimentally and theoretically. The present data agree very well in magnitude with the results of Meyer and co-workers[6,12] where they overlap in energy, and with the calculated total cross sections of Sidis and Kubach.[13]

Preliminary results are shown in Figure 8 of σ_{+o} measurements made for 1.0 and 1.5 keV D^+ on Cs ($x = 6.5 \times 10^{12}$ cm^{-2}). No corrections have been made to the data either for the finite angular width of the incident beam or the detector

resolution. Clearly, the angular distribution of product D^0 atoms at these energies is very sharply forward peaked, falling more than three orders of magnitude within 1° of the beam center. As might be expected, wide angle scattering becomes somewhat more pronounced as the collision energy is decreased.

Experiments are currently underway to measure the differential elastic scattering cross sections for $D^{+,0,-}$ in Cs at these energies where large angular effects will be most important. Additional measurements will also be made of the differential and total cross sections for several of the other major electron capture and loss processes occuring in the D-Cs system.

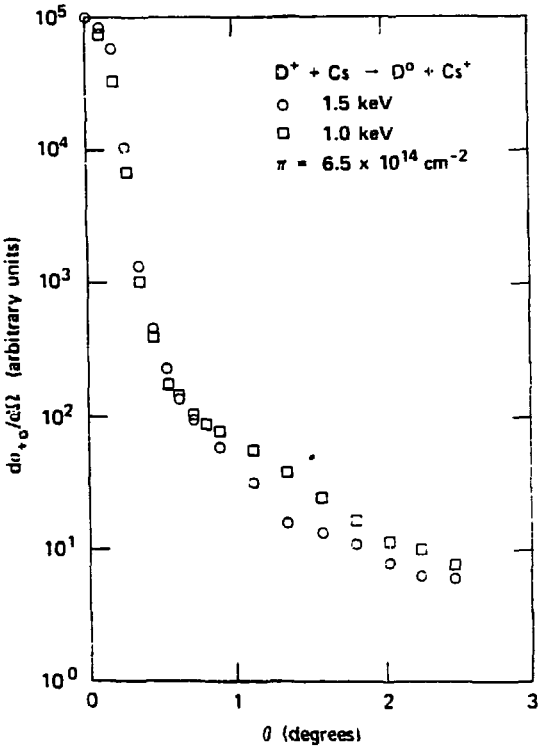

Fig. 8 Measured differential cross sections for $D^+ + Cs \rightarrow D^0 + Cs^+$ at 1.0 keV (●) and 1.1 keV (■) collision energy.

Summary

A computer model has been developed to describe the effects of angular scattering in the formation of D^- from D^+ by the two-step charge-exchange process. The model has been successfully tested in the $D^+ + Cs$ system using a combination of measured and estimated differential scattering cross sections. We have also initiated an experimental program with the goal of measuring many of the presently unknown cross sections required as input for the model. As the range of input data is extended both by experiments and in some cases accurate theoretical calculations, the model will increasingly be used to predict optimum conditions for negative ion production. Although initial work has been confined to Cs, other promising target species will be examined in the future.

Acknowledgments

This work was supported by the MFE division of the U.S. Department of Energy. The computer used in this work was purchased under NSF grant PHY76-144361.

References

1. N.F. Mott and H.S.W. Massey, "Theory of Atomic Collisions," Oxford University Press (1965), p. 470.

2. E.B. Hooper, Jr. and P.A. Willmann, J. Appl. Phys. 48, 1041 (1977).

3. C. Cisneros, I. Alvarez, C.F. Barnett and J.A. Ray, Phys. Rev. A 14, 76 (1976).

4. P. Pradel, M. El Maddarsi, and A. Valance, Chem. Phys. Lett. 71, 55 (1980); and private communication.

5. E.B Hooper, Jr., P.A. Willmann, and A.S. Schlachter, LLL Report UCID-17726 (1978).

6. F.W. Meyer, J. Phys. B, to be published.

7. A.S. Schlachter, K.R. Stalder, and J.W. Stearns, Phys. Rev. A, to be published.

8. R.E. Olson, private communication (see preceding paper in proceedings of this conference.

9. E.B. Hooper, Jr., P. Poulsen, T.A. Pincosy, O.A. Anderson, and T.J.Duffy, LBL Report in preparation, 1980.

10. Yu.A. Agafonov, B.A. Dyachkov, and M.A. Pavlii, to be published in Sov. Phys.-Tech. Phys.

11. J.R. Peterson and D.C. Lorents, Phys. Rev. 182, 152 (1969).

12. F.W. Meyer, C.J. Anderson, and L.W. Anderson, Phys. Rev. A 15, 455 (1977).

13. V. Sidis and C. Kubach, J. Phys. B 11, 2687 (1978).